

Chapter 27

High Throughput pH Optimization of Protein Crystallization

Ran Meged, Orly Dym, and Joel L. Sussman

Most high throughput structural proteomics centers use the sitting-drop method to obtain diffracting crystals for three-dimensional (3D) structure determination of biological macromolecules by x-ray crystallography. Although several robotic systems are available for dispensing the initial sitting-drop screening conditions, generally they are not used for optimization of crystallization conditions. This chapter describes a protocol for such automated systems, which permits easy construction of pH optimization grids using any desired fixed buffer set with varying ionic strengths directly dispensed into the crystallization plate.

1. Introduction

Despite technical and methodological advances, obtaining diffracting crystals remains a major obstacle to the 3D structure determination of biological macromolecules by x-ray crystallography (1). Several methods are commonly used for crystallizing proteins, including vapor diffusion, micro-batch under oil, free interface diffusion, and microdialysis. The most commonly used method is vapor diffusion, and the majority of high throughput (HTP) crystallizations centers use the sitting-drop variant (2).

Various robotic systems are available for dispensing the initial set of sitting-drop screening conditions. However, the sitting-drop method poses serious challenges to these systems:

1. Two different solution volumes are used, that of the reservoir (50–500 μL), and that of the drop (0.05–2 μL) (Fig. 27.1). Most dispensing systems for crystallization robots are adapted to utilizing very small drop volumes, so as to minimize protein consumption. For higher volumes these robots have limited capabilities, which can be overcome by the use of a more general-purpose liquid handling robot specifically designed to handle such volumes.
2. In many cases the chemicals used for crystallization, primarily the precipitants, are rather viscous (Table 27.1), rendering construction of fine and accurate gradients difficult for automated systems in terms of efficiency and accuracy (3).

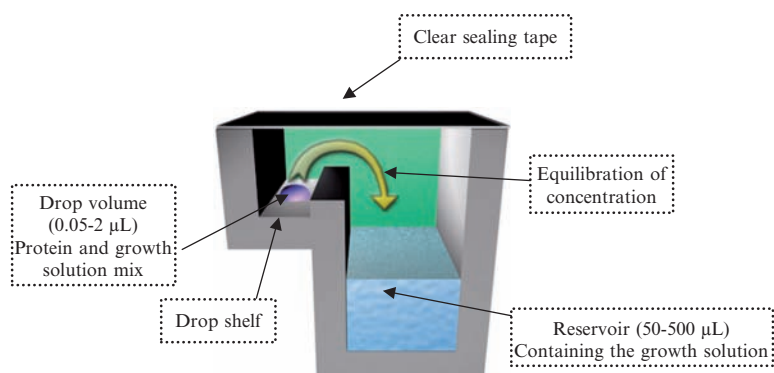


Fig. 27.1 Closed chamber for crystallization using the sitting-drop procedure: side view.

Table 27.1 Examples of liquid viscosities.

Chemical	Concentration	Viscosity, cP at 25°C
Water	100%	~1
Ethylene glycol	100%	~16
MPD (2-methyl-2,4-pentanediol)	100%	~36
PEG 200 (polyethylene glycol)	100%	~50
PEG-1000	50%	~20
PEG-4000	50%	~100

Once a protein crystal is grown from a given set of screening conditions, whether commercial or “in house,” its diffraction pattern is measured, and an x-ray data set at cryogenic temperature is normally collected. For poorly diffracting protein crystals, with a resolution, e.g., worse than approximately 3Å, both crystal growth and freezing conditions need to be optimized (4) to improve diffraction quality. Furthermore, optimization can produce crystals of larger dimensions, and may also increase the probability of obtaining single crystals. Many variables that affect crystal quality can potentially be optimized, including:

1. The protein sequence (mutations, truncations, etc.), purity, concentration, or presence of inhibitors or cofactors
2. Optimization of the initial “hit solution” (5), i.e., the crystallization conditions for the initial crystal *hits*, which include a precipitant, a buffer, and often a salt, an additive, and a detergent
3. Thermodynamic parameters, including, in particular, temperature (2,3,6,7)

The most convenient ways for optimizing the initial “hit solution” are either varying the pH, or varying the precipitant concentration (8) (which can lead to the construction of the phase diagram) (Fig. 27.2).

The authors have developed a pH optimization protocol designed for automated systems that is easy to use, thus making it very suitable for HTP optimization following initial screening.

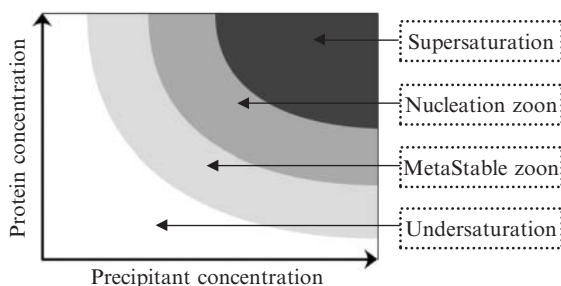


Fig. 27.2 Phase diagram plotting the solubility curve of a protein. The horizontal axis shows the parameter varied, usually the precipitant concentration. The vertical axis shows the protein concentration.

2. Materials

2.1. Apparatus

1. Liquid-handling robot with an eight-tip dispensing arm, suitable for use with either fixed or disposable tips.
2. Robotic stage capable of accepting at least four SBS plates (see [Note 1](#)).
3. Three polypropylene 96-well master blocks with a well volume of 2 ml.
4. One SBS sitting-drop crystallization plate.
5. Transparent sealing tape.
6. An eight-channel multi-pipettor (optional).

2.2. Stock Solutions

1. Suggested buffer solutions ([Table 27.2](#)) with two extreme ionic strengths.

3. Methods

3.1. Preparation of Buffer Stocks

1. Select specific buffers (see [Table 27.2](#)).
2. Prepare two solutions of minimal and maximal pH.
3. Set up the pH gradient according to the crystallization plates being used (see [Table 27.2](#) for suggestions).
4. Generate the desired pH by mixing appropriate volumes of the two extreme pH buffers (see [Note 2](#)). A liquid-handling robot can construct such plates quite easily because the viscosities of all the buffers are close to that of water.

3.2. Optimization of the Hit Growth Solution

1. Prepare a solution for optimizing crystal growth, i.e., a *hit growth solution* ([Fig. 27.3A,B](#)).
2. Select buffers with pH values that are most compatible with the hit solution, and dispense them, using appropriate gradients closest to the hit value, as illustrated in [Table 27.1](#) and [Fig. 27.3C](#).

Table 27.2 Suggested buffer compositions, gradients, concentrations and configurations.

Deep Well 1:					
Buffer	Min	Max	Conc (M)	pKa (at ~20°)	
Na-acetate	4.5	5.5	1	4.76	
	5.5	6.5	1	4.76	
Imidazole-maleate	4.5	5.5	1	7.05	
	5.5	6.5	1	7.05	
	6.5	7.5	1	7.05	
	7.5	8.5	1	7.05	
Na-cacodylate	4.5	5.5	1	6.27	
	5.5	6.5	1	6.27	
	6.5	7.5	1	6.27	
Na-citrate	4.5	5.5	1	4.76	
	5.5	6.5	1	4.76	
	6.5	7.5	1	4.76	

	1	2	3	4	5	6	7	8	9	10	11	12	
<i>A</i>	4.5	5.5	4.5	5.5	6.5	7.5	4.5	5.5	6.5	4.5	5.5	6.5	
<i>B</i>	4.6	5.6	4.6	5.6	6.6	7.6	4.6	5.6	6.6	4.6	5.6	6.6	
<i>C</i>	4.8	5.8	4.8	5.8	6.8	7.8	4.8	5.8	6.8	4.8	5.8	6.8	
<i>D</i>	4.9	5.9	4.9	5.9	6.9	7.9	4.9	5.9	6.9	4.9	5.9	6.9	
<i>E</i>	5.1	6.1	5.1	6.1	7.1	8.1	5.1	6.1	7.1	5.1	6.1	7.1	
<i>F</i>	5.2	6.2	5.2	6.2	7.2	8.2	5.2	6.2	7.2	5.2	6.2	7.2	
<i>G</i>	5.4	6.4	5.4	6.4	7.4	8.4	5.4	6.4	7.4	5.4	6.4	7.4	
<i>H</i>	5.5	6.5	5.5	6.5	7.5	8.5	5.5	6.5	7.5	5.5	6.5	7.5	
	Na-acetate						Na-cacodylate						Na-citrate

Deep Well 2:	Min	Max	Conc (M)	pKa (at -20°)
Buffer				
BisTriPro	6.5	7.5	1	6.8
	7.5	8.5	1	6.8
	8.5	9.5	1	6.8
HEPES	6.5	7.5	1	7.55
	7.5	8.5	1	7.55
TRIS-HCl	7.0	8.5	1	8.1
Na-Tricine	7.5	8.5	1	8.16
HEPPO	7.5	8.5	1	7.8
CAPSO	8.5	9.5	0.5	9.6
AMPPO	8.5	9.5	1	9
CHES	8.5	10.0	1	9.55
CAPS	10.0	11.0	1	10.56

	1	2	3	4	5	6	7	8	9	10	11	12
A	6.5	7.5	8.5	6.5	7.5	7.0	7.5	7.5	8.5	8.5	8.5	10.0
B	6.6	7.6	8.6	6.6	7.6	7.2	7.6	7.6	8.6	8.6	8.7	10.1
C	6.8	7.8	8.8	6.8	7.8	7.4	7.8	7.8	8.8	8.8	8.9	10.3
D	6.9	7.9	8.9	6.9	7.9	7.6	7.9	7.9	8.9	8.9	9.1	10.4
E	7.1	8.1	9.1	7.1	8.1	7.9	8.1	8.1	9.1	9.1	9.4	10.6
F	7.2	8.2	9.2	7.2	8.2	8.1	8.2	8.2	9.2	9.2	9.6	10.7
G	7.4	8.4	9.4	7.4	8.4	8.3	8.4	8.4	9.4	9.4	9.8	10.9
H	7.5	8.5	9.5	7.5	8.5	8.5	8.5	8.5	9.5	9.5	10.0	11.0
	BisTriPro			HEPES		TRIS-HCl	Na-Tricine	HEPPO	CAPSO	AMPPO	CHES	CAPS

(continued)

Table 27.2 (continued)

Deep Well 3:	Min	Max	Conc (M)	pKa (at ~20°)
Buffer				
TRIS-maleate	4.5	5.5	1	6.26
	5.5	6.5	1	6.26
Na-succinate	4.5	5.5	1	4.19
	5.5	6.5	1	4.19
	6.5	7.5	1	4.19
Na-K-phosphate	5.5	6.5	1	7.21
	6.5	7.5	1	7.21
	7.5	8.5	1	7.21
MES	5.5	6.5	1	6.16
BisTRIS	5.5	7.0	1	6.5

	I	2	3	4	5	6	7	8	9	10
A	4.5	5.5	4.5	5.5	6.5	5.5	6.5	7.5	5.5	5.5
B	4.6	5.6	4.6	5.6	6.6	5.6	6.6	7.6	5.6	5.7
C	4.8	5.8	4.8	5.8	6.8	5.8	6.8	7.8	5.8	5.9
D	4.9	5.9	4.9	5.9	6.9	5.9	6.9	7.9	5.9	6.1
E	5.1	6.1	5.1	6.1	7.1	6.1	7.1	8.1	6.1	6.4
F	5.2	6.2	5.2	6.2	7.2	6.2	7.2	8.2	6.2	6.6
G	5.4	6.4	5.4	6.4	7.4	6.4	7.4	8.4	6.4	6.8
H	5.5	6.5	5.5	6.5	7.5	6.5	7.5	8.5	6.5	7.0
	TRIS-maleate			Na-succinate				Na-K-phosphate	MES	BisTRIS

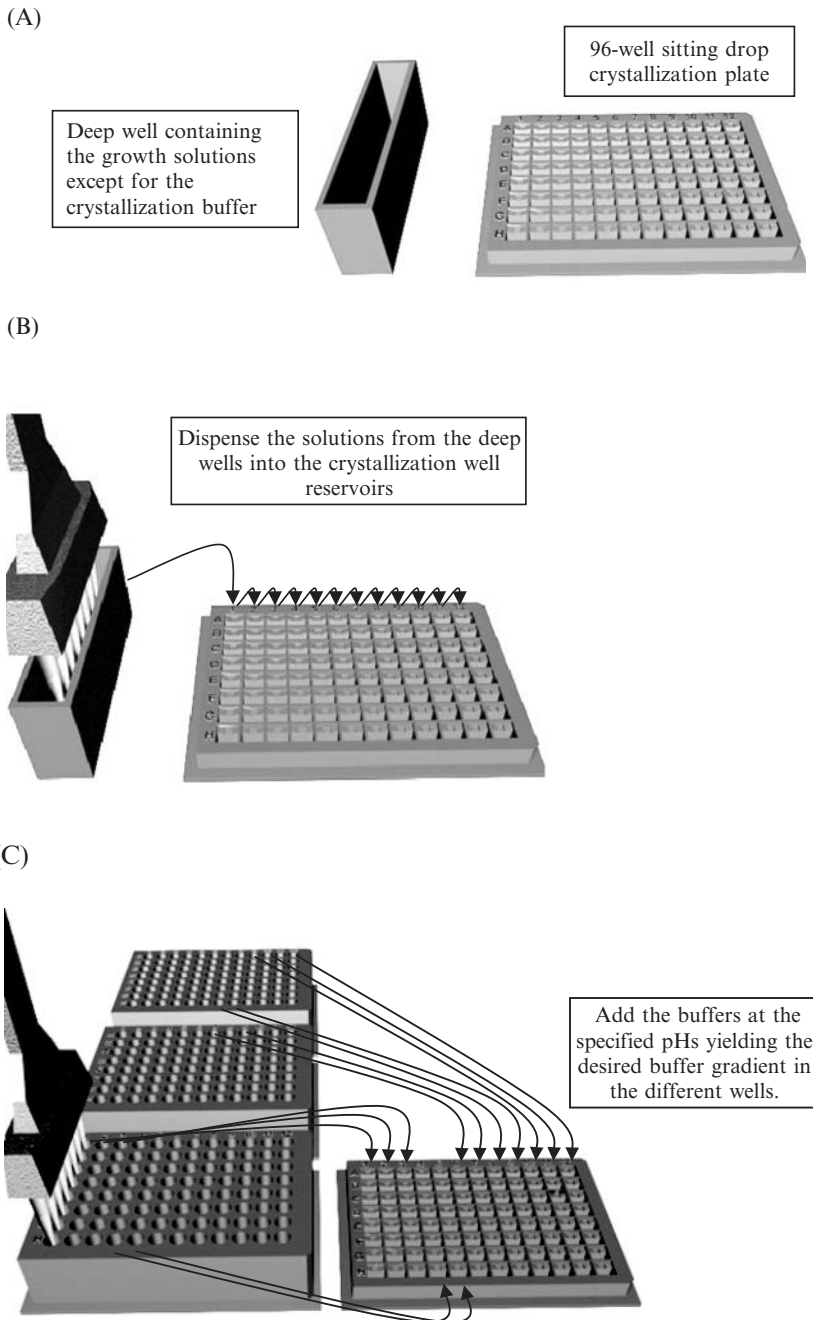


Fig. 27.3 Schematic illustration of the use of a liquid-handling robot to prepare the optimized crystallization growth solutions. **A.** Growth solutions dispensed into the deep well with the exception of the crystallization buffer. **B.** Dispense the solutions from the deep wells (A) into the crystallization well reservoirs. **C.** Add the buffers at the specified pHs yielding the desired buffer gradient in the different wells.

3. Dispense the protein and the reservoir solution together onto the drop shelf (see Fig. 27.1), cover the plate with sealing tape, and store at the desired temperature.

4. Notes

1. The standards dimensions and tolerance for crystallization plates are compiled by the Microplate Standards Working Group of the Society for Biomolecular Sciences and can be found at www.sbsonline.org/msdc/approved.php
2. Ratio of the volumes of the two buffers

The ratio of the volumes of the two buffers needed to achieve a given pH value is calculated using the Henderson-Hasselbach equation:

$$\text{pH} = \text{pka} + \log_{10}([\text{salt}]/[\text{acid}])$$

which can be rewritten:

$$[\text{salt}][\text{H}] - \text{Ka}[\text{acid}] = 0$$

Acknowledgments

The authors acknowledge a grant from The Israel Ministry of Science, Culture and Sport to the ISPC, and the support of the Divadol Foundation, the Newman Foundation, and the European Commission Sixth Framework Research and Technological Development Programme SPINE2-COMPLEXES Project under contract No. 031220. The authors thank Israel Silman for his critical reading of the manuscript. J. L. Sussman is the Morton and Gladys Pickman Professor of Structural Biology.

References

1. Bränden, C., and Tooze, J. (1999) *Introduction to Protein Structure*, Garland Publishing, New York.
2. McPherson, A. (1990) Current approaches to macromolecular crystallization. *Eur. J. Biochem.* **189**, 1–23.
3. Ducruix, A., and Giegé, R. (Eds.) (1999) *Crystallization of Nucleic Acids and Proteins: A Practical Approach*, Oxford University Press, Oxford, UK.
4. Chayen, N. E., and Saridakis, E. (2002) Protein crystallization for genomics: towards high throughput optimization techniques. *Acta Cryst.* **D58**, 921–927.
5. Leulliot, N., Tresaugues, L., Bremang, M., Sorel, I., Ulryck, N., Graille, M., Aboulfath, I., Poupon, A., Liger, D., Quevillon-Cheruel, S., Janin, J., and van Tilbeurgh, H. (2005) High throughput crystal-optimization strategies in the South Paris Yeast Structural Genomics Project: one size fits all? *Acta Cryst.* **D61**, 664–670.
6. Giegé, R., and Mikol, V. (1989) Crystallogenesis of proteins. *Trends Biotechnol.* **7**, 277–282.
7. Lorber, B., and Giegé, R. (1992) A versatile reactor for temperature controlled crystallization of biological macromolecules. *J. Cryst. Growth* **122**, 168–175.
8. Shaw Stewart, P. D., and Baldock, P. F. M. (1999) Practical experimental design techniques for automatic and manual protein crystallization. *J. Cryst. Growth* **196**, 665–673.